Eur. Phys. J. A **2**, 383–390 (1998)

THE EUROPEAN PHYSICAL JOURNAL A

Spectator Nucleons in Pb+Pb Collisions at 158 A·GeV

H. Appelshäuser[7], J. Bächler[5], S.J. Bailey[16], L.S. Barnby[3], J. Bartke[6], R. A. Barton[3], H. Białkowska[14], C.O. Blyth[3], R. Bock[7], C. Bormann[10], F.P. Brady[8], R. Brockmann[7,g], N. Buncic[5,10], P. Buncic[5,10], H.L. Caines[3], D. Cebra[8], P. Chan[16], G.E. Cooper[2], J.G. Cramer[16,13], P.B. Cramer[16], P. Csato[4], J. Dunn[8], V. Eckardt[13], F. Eckhardt[12], M.I. Ferguson[5], H.G. Fischer[5], D. Flierl[10], Z. Fodor[4], P. Foka[10], P. Freund[13], V. Friese[12], M. Fuchs[10], F. Gabler[10], J. Gal[4], M. Gaździcki[10], E. Gładysz[6], P. Gorodetsky[f], J. Grebieszkow[15], J. Günther[10], J.W. Harris[17], S. Hegyi[4], T. Henkel[12], L.A. Hill[3], I. Huang[2,8], H. Hümmler[10], G. Igo[11], D. Irmscher[2,7,a], P. Jacobs[2], P.G. Jones[3], K. Kadija[18,13], V.I. Kolesnikov[9], M. Kowalski[6], B. Lasiuk[11,h], P. Lévai[4], A.I. Malakhov[9], S. Margetis[2,c], C. Markert[7], G.L. Melkumov[9], A. Mock[13], J. Molnár[4], J.M. Nelson[3], G. Odyniec[2], G. Palla[4], A.D. Panagiotou[1], A. Petridis[1], A. Piper[12], R.J. Porter[2], A.M. Poskanzer[2,b], S. Poziombka[10], D.J. Prindle[16], F. Pühlhofer[12], W. Rauch[13], J.G. Reid[16], R. Renfordt[10], W. Retyk[15], H.G. Ritter[2], D. Röhrich[10], C. Roland[7], G. Roland[10], H. Rudolph[2,10], A. Rybicki[6], I. Sakrejda[2], A. Sandoval[7], H. Sann[7], A.Yu. Semenov[9], E. Schäfer[13], D. Schmischke[10], N. Schmitz[13], S. Schönfelder[13], P. Seyboth[13], J. Seyerlein[13], F. Sikler[4], E. Skrzypczak[15], G.T.A. Squier[3], R. Stock[5,10], H. Ströbele[10], I. Szentpetery[4], J. Sziklai[4], M. Toy[2,11], T.A. Trainor[16], S. Trentalange[11], T. Ullrich[17], M. Vassiliou[1], G. Vesztergombi[4], D. Vranic[7,18], F. Wang[2], D.D. Weerasundara[16], S. Wenig[5], S. White[e], C. Whitten[11], T. Wienold[2,a,d], L. Wood[8], T.A. Yates[3], J. Zimanyi[4], X.-Z. Zhu[16], R. Zybert[3]
NA49 Collaboration

[1] Department of Physics, University of Athens, Athens, Greece
[2] Lawrence Berkeley National Laboratory, University of California, Berkeley, USA
[3] Birmingham University, Birmingham, England
[4] KFKI Research Institute for Particle and Nuclear Physics, Budapest, Hungary
[5] CERN, Geneva, Switzerland
[6] Institute of Nuclear Physics, Cracow, Poland
[7] Gesellschaft für Schwerionenforschung (GSI), Darmstadt, Germany
[8] University of California at Davis, Davis, USA
[9] Joint Institute for Nuclear Research, Dubna, Russia
[10] Fachbereich Physik der Universität, Frankfurt, Germany
[11] University of California at Los Angeles, Los Angeles, USA
[12] Fachbereich Physik der Universität, Marburg, Germany
[13] Max-Planck-Institut für Physik, Munich, Germany
[14] Institute for Nuclear Studies, Warsaw, Poland
[15] Institute for Experimental Physics, University of Warsaw, Warsaw, Poland
[16] Nuclear Physics Laboratory, University of Washington, Seattle, WA, USA
[17] Yale University, New Haven, CT, USA
[18] Rudjer Boskovic Institute, Zagreb, Croatia

Received: 16 February 1998 / Revised version: 30 March 1998
Communicated by V. Metag

Abstract. The composition of forward-going projectile spectator matter in fixed-target Pb+Pb collisions at 158 A·GeV at the CERN SPS has been studied as a function of centrality. The data were measured with the NA49 veto calorimeter. We observe that forward-going spectator matter in central collisions consists of 9 neutrons, 7 protons, and half a deuteron on average. At large impact parameters most spectator nucleons are bound in fragments. The relative resolution of the average impact parameter derived from the measurement of spectator neutrons is roughly 19% in the range from zero to half maximum impact parameters.

PACS. 25.75.-q Relativistic heavy-ion collisions

[a] Alexander von Humboldt Foundation (Lynen) Fellow
[b] Alexander von Humboldt Foundation U.S. Senior Scientist Award Recipient
[c] *Present address:* Kent State University, Kent, OH, USA
[d] *Present address:* Physikalisches Institut, Universität Heidelberg, Germany
[e] *Address:* Brookhaven National Laboratory, Upton, N.Y., U.S.A
[f] *Address:* College de France, Paris, France
[g] deceased
[h] *Present address:* Yale University, New Haven, CT, USA

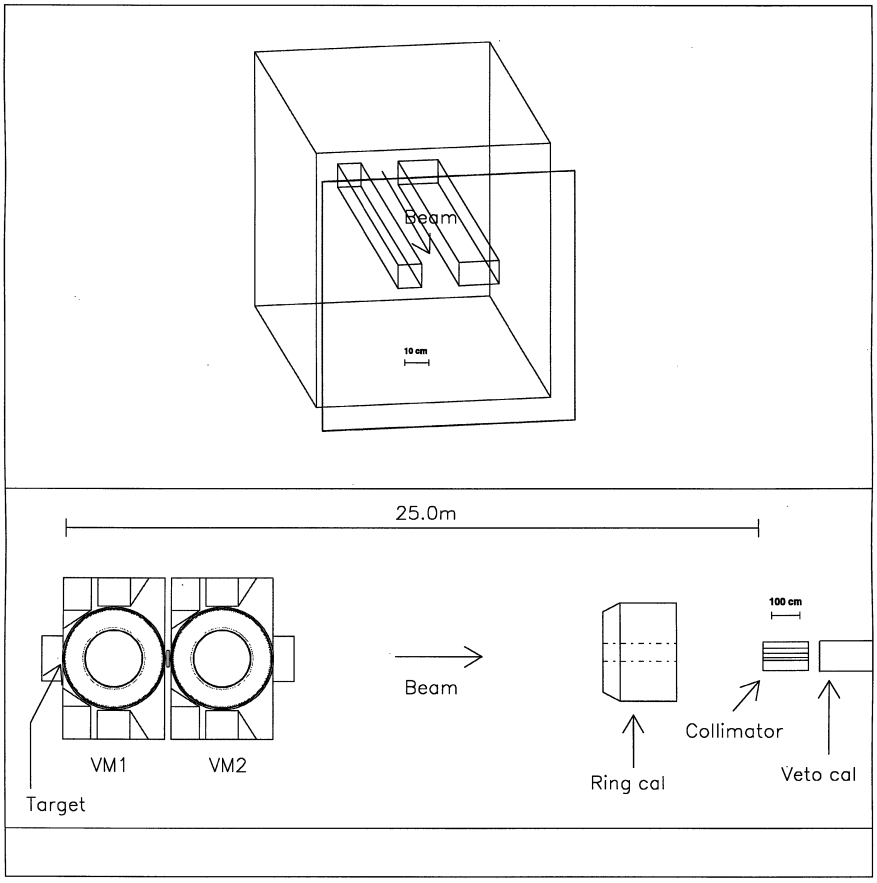

Fig. 1. Upper: A view of the collimator configured to accept spectator nucleons. Lower: A fragmentation run setup. Only the relevant detectors are depicted. The target is 25 m upstream of the front face of the collimator. Two Vertex Magnets (VM) are used to separate particles of different charge-to-mass ratios. The ring calorimeter measures the energy in the laboratory pseudorapidity range of $3.2 < \eta < 4.9$ in the vertical plane. The forward-going energy within the acceptance of the collimator is measured in the veto calorimeter

1 Introduction

In heavy ion experiments, forward-going particles are often used for on-line triggering. In a simple geometrical picture, forward-going matter reflects the degree of centrality of each event. The more central a collision is, the fewer fast particles enter a forward region of small solid angle around the beam. In peripheral collisions, a large fraction of the beam energy remains in the forward region [1].

Projectile fragmentation in heavy ion collisions has been studied [2,3] at Bevalac energies. The cross sections for the emission of fragments, which can result from the strong nuclear interaction or the electromagnetic interaction, depend on the impact parameter of the collision. When fragmentation is caused by the nuclear interaction, the cross sections are strongly dependent on the geometry of the collision. According to the hypothesis of limiting fragmentation [4], these cross sections and spectra have little beam energy dependence above kinetic energies of about a hundred A·MeV. There are experimental confirmations of this hypothesis [5,6]. Within the scenario of limiting fragmentation, the fragmentation of forward-going projectile matter at SPS energies ($\approx$ 160 – 200 A·GeV) would be similar to those which have been measured at the Bevalac [7,8] ($\approx$ 1 A·GeV), SIS [9,10] ($\approx$ 0.1 – 1 A·GeV), and AGS [11,12] ($\approx$ 10 A·GeV) energies. Indeed fragments with mass numbers close to the one of the projectile have been observed in peripheral heavy-ion collisions involving light projectile nuclei (oxygen and sulphur) at 200 A·GeV [13,14], however, the reported cross sections are smaller than predicted by limiting fragmentation at 200 A·GeV [13].

For better understanding of the Pb+Pb reaction mechanism, it is important to investigate the composition of the spectator matter which consists of nucleons and nuclei. In this work we study the composition of spectator matter in terms of bound and free nucleons as a function of impact parameter. We define spectator nucleons by requiring that their momentum in the projectile rest frame is below 270 MeV/c.

2 Experimental setup

The experimental setup of the NA49 fragmentation run is shown in Fig. 1. It uses two superconducting dipole Vertex Magnets (VM1 & VM2) with a total bending power of 7.8 T·m immediately downstream of the target to bend the trajectories of charged particles in the horizontal (bending) plane. In the fragmentation region where every nucleon has approximately the beam energy per nucleon, the deflections of charged particles depend mainly on their charge-to-mass (Z/A) ratios (apart from the spread due to the Fermi momentum). At a distance of 25 m from the target, where the front face of the collimator is posi-

tioned, the average horizontal deflection of charged particles from the undeflected beam trajectory is 11.9 cm for the ^{208}Pb nuclei (Z/A=0.39), 15.1 cm for the particles with $Z/A = 1/2$, and 30.3 cm for protons, as shown in Fig. 2.

The NA49 setup is equipped with two calorimeters: the ring calorimeter (Ring Cal) and veto calorimeter (Veto Cal). Ring Cal consists of an electromagnetic lead-scintillator calorimeter of 16 radiation lengths (1 interaction length), followed by a hadronic iron-scintillator calorimeter of 6 interaction lengths. It is a barrel that has an inner/outer radius of 0.28/1.50 meters. Ring Cal measures the energy (E_R) with an overall relative energy resolution ($\sigma(E_R)/E_R$) of about $100\%/\sqrt{E_R}$ (E_R in GeV) in the laboratory pseudorapidity range of $3.2 < \eta < 4.9$ for neutral particles. Since the charged particle trajectories are bent by the magnetic field the phase space seen by Ring Cal is a complex function of rapidity and transverse momentum, but the total energy per event detected by the Ring Cal is still a good measure of the centrality of the collision. The projectile spectator matter is found at small angles not covered by Ring Cal and travels through its hole to Veto Cal.

The energy (E_V) of the forward-going spectator matter is measured in the veto calorimeter. It is a lead-iron/scintillator hadronic calorimeter with a total of 10 interaction lengths. Its relative energy resolution is about $200\%/\sqrt{E_V}$ (E_V in GeV). It was calibrated with the Pb beam of energy 32.9 TeV. The acceptance of Veto Cal is defined by the opening of the iron collimator positioned immediately upstream of Veto Cal. The size and position of the opening(s) are adjustable. The full opening, 43 cm wide in the horizontal direction and 10 cm in the vertical direction, is sufficient to accept the spectator neutrons, protons, and fragments, including their spread due to Fermi momentum. The collimator opening can be adjusted to different sizes (see Fig. 2) to accept various spectator species in separate runs. As illustrated, the possible configurations are labeled 'neutron', 'proton', 'nucleon' (i.e. neutron+proton), 'fragment', and 'all spectator' (i.e. neutron+proton+fragment). In each configuration, sufficient amounts of data without a target (target-out runs) were collected in order to estimate the effect of the background.

Two target thicknesses—2.0% and 0.5% of the Pb+Pb interaction length—and two trigger configurations were employed. In the minimum bias mode, a gas Čerenkov detector positioned a few centimeters downstream of the target was used to veto non-interacting Pb-beam particles. In this mode, the ratio of target-out to target-in interactions for the 2.0% target was about 1/5. The background resulted from interactions of Pb particles with low Z material in the upstream part of the beam line. It is suppressed by the second trigger (medium bias) condition which requires an energy larger than ≈ 4 TeV in the ring calorimeter. The ratio of target-out interactions to target-in interaction with an off-line centrality cut of $E_R > 6$ TeV is 8% for the thick target and 28% for the thin target. Whenever necessary, the background was subtracted in the analysis presented below.

3 Data analysis

The correlation of the energy measured in Veto Cal (E_V) as a function of E_R measured in Ring Cal for events obtained with a minimum bias trigger is displayed in Fig. 3 for three different collimator configurations (see Fig. 2). The data collected in the 'Fragment' (upper panel) and 'Nucleon' (lower panel) are represented by the boxes whereas in both panels the 'All spectator' configuration results are shown as crosses. Qualitatively, all correlations can be understood within a participant-spectator picture. In central collisions, many nucleons collide resulting in a multitude of produced particles, which deposit their energy in Ring Cal, and only a few spectators remain. In peripheral collisions, a large number of spectator nucleons and fragments deposit a substantial fraction of the incoming beam energy in Veto Cal and there is only little energy from produced particles seen in Ring Cal. The fragments show a similar behavior as all spectators (upper panel) whereas the energy in the nucleons (lower panel) reaches a maximimum at intermediate energies in the ring calorimeter.

The lower E_R region (< 6 TeV) is increasingly contaminated by Pb+air interactions the contribution of which was quantified in target-out runs and subtracted wherever appropiate. In order to increase statistics on valid Pb+Pb interactions, data with medium bias trigger (defined in the previous chapter) were taken in all collimator configurations.

In order to obtain information about the number of spectator nucleons from the measured energies in the veto calorimeter one has to correct for the contributions from other sources. These non-spectator contributions are due to energy leaking out from the back of the collimator and

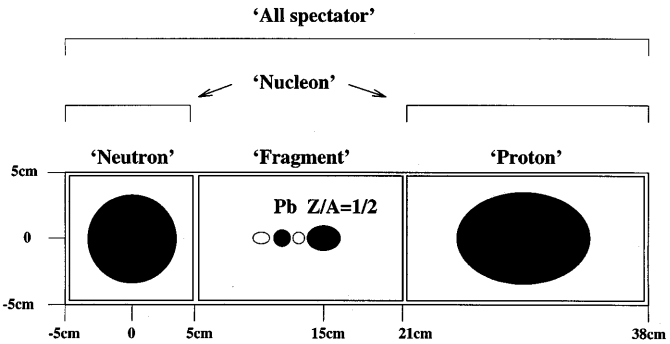

Fig. 2. An illustration of the horizontal deflection of charged particles at the front face of the iron collimator. The broadened distribution of each species is due to the Fermi motion of nucleons or fragments; additionally, the oval shapes are due to the deflection of charged particles in the magnetic field. The sizes of the distributions correspond to one standard deviation. The open circles in the fragment acceptance represent particles of Z/A other than one half

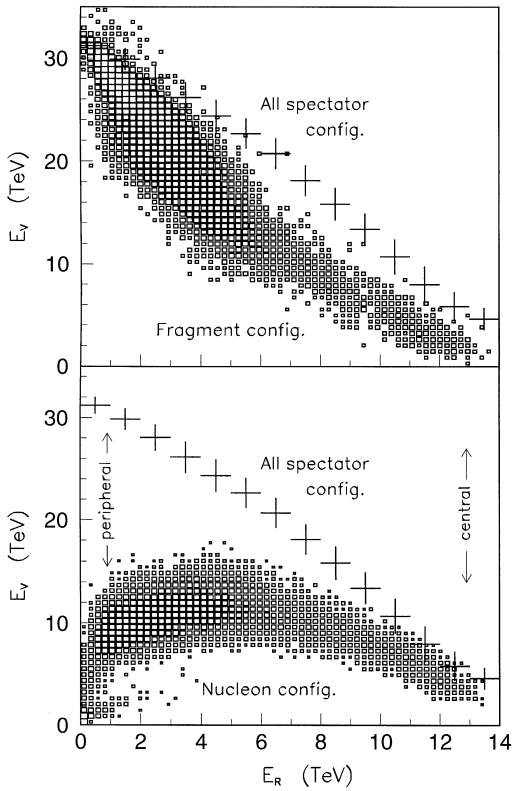

Fig. 3. Upper: The energy measured in Veto Cal with the open collimator (crosses) and with the 'fragment' configuration (boxes) as a function of the energy measured in Ring Cal. Lower: The same correlation with the 'nucleon' configuration. The central Pb+Pb collisions are characterized by high E_R, and the peripheral collisions by low E_R

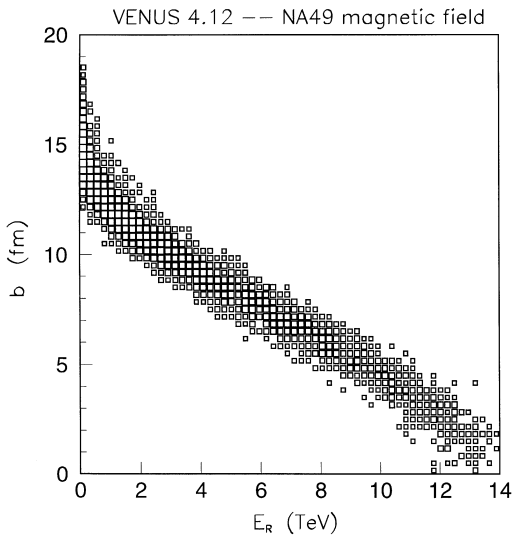

Fig. 4. VENUS simulation of the correlation between impact parameter and the energy seen by the ring calorimeter E_R with the NA49 magnetic field on

Table 1. E_R bins and their corresponding average impact parameter values and their spread in RMS values

E_R (TeV)			$\langle b \rangle$ (fm)		
12	–	14	2.1	±	0.9
10	–	12	3.7	±	0.9
8	–	10	5.4	±	0.7
6	–	8	6.9	±	0.7
4	–	6	8.4	±	0.7
2	–	4	10.5	±	0.8
0	–	2	13.4	±	1.5

energy of participating nucleons as well as produced particles which pass through the various openings of the collimator. The latter consist mainly of neutral particles from the primary interaction and include particles from secondary interactions in the air. The corrections were computed using the GEANT code [15] to simulate particle trajectories. The input to the simulation was derived from the event generator VENUS [16] (version 4.12) which, however, does not generate any fragments. All spectator nucleons are treated as free nucleons with beam energy and zero transverse momentum. In order to simulate fragmentation A/Z=2 nuclei were formed according to the following prescription which is based on a comparison of the energy in the veto calorimeter as given by the VENUS code with what is measured in the 'Neutron' configuration for a given E_R interval. The difference between VENUS prediction for spectator neutrons and measurement is attributed to those spectator neutrons which are bound in fragments and are therefore deflected away from the 'Neutron' opening of the collimator. These excess neutrons are combined with an equal number of spectator protons to become deuterons (or other Z/A=0.5 fragments) The multiplicity and Z/A ratio of the formed fragments are not important since Veto Cal cannot distinguish the energy carried by a fragment of atomic number A from the sum of energies carried by a collection of smaller fragments whose nucleon numbers add up to A. In this way, the GEANT output is made to match the measured neutron data and provides a reasonable estimate of the contributions from non-spectator sources to the energy measured by the veto calorimeter in the different collimator configurations.

The VENUS simulation provides a distribution of the impact parameters (b) for a given value of E_R. Fig. 4 shows the corresponding correlation. $\langle b \rangle$ and its RMS width in 2 TeV bins of E_R are given in Table 1 for the whole range of energies obtained from the ring calorimeter.

In the simulation, the total energy deposited in the veto calorimeter through the particular collimator openings consists of the spectator part (which is denoted E_{input}^{spec}) and the non-spectator part, which is composed of the leakage through the collimator and the energies carried by produced particles and participant nucleons. The latter are defined to be those that have momenta greater than 270 MeV/c in the projectile rest frame (Veto Cal accepts protons with momenta smaller than 315 MeV/c in the same Lorentz-frame; for neutrons the same cut applies to their transverse momenta). The essential information in the simulation is the fraction of the total energy (E_{VETO}) which is due to spectator nucleons and fragments (E_{input}^{spec}).

Table 2. GEANT simulation of fragmentation (Energy in TeV). The ratio of E^{spec}_{input} to E_{VETO} is the correction factor to be applied to raw data. ⟨# spec⟩ is the average number of nucleons in each spectator species expected to be within the acceptance, and their errors are RMS values. ⟨# prtcp⟩ is the average number of participant nucleons expected to be within the acceptance

⟨b⟩ (fm)	E^{spec}_{input}	/ E_{VETO} =	Factor (%)	⟨# spec⟩	⟨# prtcp⟩
Total					
2.0	2.55	4.53	56	16.2 ± 5.2	11.1
4.0	5.48	7.72	71	34.7 ± 10	13.1
5.8	9.87	12.4	79	62.5 ± 12	15.0
7.6	15.0	17.4	86	95.3 ± 13	14.5
9.1	19.3	21.1	91	122 ± 14	12.4
11.2	25.3	25.9	98	160 ± 12	8.1
Fragment					
2.0	0.12	1.04	11	0.8 ± 1.3	4.1
4.0	1.09	2.13	51	6.9 ± 2.8	4.2
5.8	2.84	4.14	69	18.0 ± 3.8	4.4
7.6	5.48	6.83	80	34.7 ± 5.3	3.7
9.1	8.45	9.74	87	53.5 ± 10.8	2.9
11.2	13.4	14.5	92	84.7 ± 14.6	1.8
Nucleon					
2.0	2.43	3.70	66	15.4 ± 5.2	7.0
4.0	4.39	5.94	74	27.8 ± 8.8	8.9
5.8	7.03	8.81	80	44.5 ± 11.4	10.6
7.6	9.57	11.4	84	60.6 ± 11.3	10.8
9.1	10.8	12.0	90	68.7 ± 11.6	9.5
11.2	11.9	12.5	95	75.2 ± 10.2	6.3
Neutron					
2.0	1.44	2.31	62	9.1 ± 3.3	4.3
4.0	2.73	3.73	73	17.3 ± 6.1	5.2
5.8	4.39	5.61	78	27.8 ± 7.9	6.5
7.6	5.94	7.25	82	37.6 ± 8.1	6.6
Proton					
2.0	0.99	1.66	60	6.3 ± 3.0	2.8
4.0	1.72	2.60	66	10.9 ± 4.3	3.7
5.8	2.67	3.67	73	16.9 ± 5.6	4.2
7.6	3.66	4.73	77	23.2 ± 5.6	4.2

The results of the simulation are summarized in Table 2. The ratios between E^{spec}_{input} and E_{VETO} are the correction factors which we applied to the values of the measured energies in the veto calorimeter in the different configurations.

After correction for the non-spectator contribution to the measured forward energies the sum of spectator neutron, proton, and fragment energies exceeded the total forward-going spectator energy in each bin (by approximately 20%), i.e. $E^c_{neutron}+E^c_{proton}+E^c_{fragment} > E^c_{all}$ where $E^c_{neutron}$, E^c_{proton}, $E^c_{fragment}$, E^c_{all} are the energies in spectator neutrons, protons, fragments, and all spectators, respectively. We conclude that the simulation does not treat correctly the energy contributed by the particles which participated in the collision. The effect is most pronounced in central collisions and may be either due to shortcomings of the event generator and/or of the GEANT code. In order to do a first order correction the following method was adopted. The final corrected neutron ($E^f_{neutron}$) and proton (E^f_{proton}) energies were determined from the corrected nucleon energy ($E^c_{nucleon}$) by the following equations:

$$E^f_{neutron} = E^c_{nucleon} \cdot E^c_{neutron}/(E^c_{neutron} + E^c_{proton}) \quad (1)$$

$$E^f_{proton} = E^c_{nucleon} \cdot E^c_{proton}/(E^c_{neutron} + E^c_{proton}) \quad (2)$$

The correction of $E^c_{fragment}$ is small because the number of nucleons in the fragments is much smaller than the number of free nucleons in central collisions. At larger impact parameters where both numbers become comparable the energy in the participants is small. With this method, the disagreement between E^c_{all} and $E^f_{neutron}+E^f_{proton}+E^c_{fragment}$ is smaller than 9%. By comparing the $E^c_{nucleon}$ and $E^c_{neutron}+E^c_{proton}$, the systematic error that cannot be accounted for by the simulation is found to be 20%.

4 Results and discussion

The differential cross sections for the corrected energy distributions with a cut $E_R > 6$ TeV for all the configurations are shown in Fig. 5. The energy measured in the "all" configuration has the widest distribution. The measurement of the fragments shows a large cross section near zero E_V. This means that in central collisions only few fragments are formed over a substantial range of impact parameters. A comparison of the neutron and (unbound) nucleon energy distributions shows that the sum of proton and neutron energies has a significantly wider distribution than the energy of the neutrons alone. This difference quantifies the increase in resolution of a centrality measurement derived from all unbound nucleons as compared to a measurement of the neutrons alone.

From the corrected neutron and proton data, the neutron-to-proton (n/p) ratio of the (unbound) spectator nucleons was found for each centrality bin as shown in Table 3. The errors in the table are estimates based on the systematic error of 20%. The n/p ratio in the ^{208}Pb projectile is 126/82=1.54. In the two most central bins the n/p ratio is slightly smaller, although by less than the quoted errors, than that of the ^{208}Pb projectile. We expect this ratio to be close to 1.54, since there are almost no fragments in central collisions. With increasing impact parameter the number of fragments increases. The large majority of these light nuclei have equal numbers neutrons and protons. We expect the overall n/p ratio (including free and bound nucleons) in spectator matter to be the same as in the Pb-nucleus. This means that the remaining free nucleons must have n/p>1.54 which is indeed observed (see Table 3). Thus the ratio of free neutrons to protons increases with and up to intermediate impact parameters. For peripheral collisions the n/p ratio will be ill defined because of the uncertainty in the fragment size and Z/A ratio.

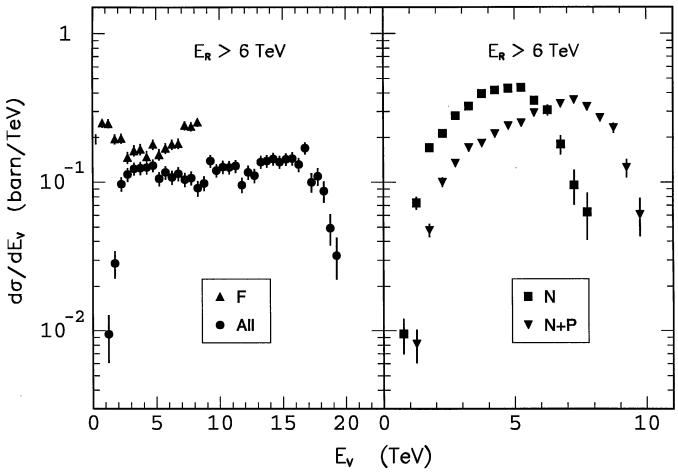

Fig. 5. The differential cross sections for the corrected energies measured with the 'all spectator', 'fragment', 'nucleon', and 'neutron' configurations with a cut of $E_R > 6$ TeV

Table 3. Neutron-to-proton ratio of spectator nucleons as a function of the impact parameter. The errors are estimated from systematic uncertainties

$\langle b \rangle$ (fm)	2.1	3.7	5.4	6.9	8.4
n/p	1.3±0.3	1.4±0.3	1.7±0.2	1.9±0.3	1.9±0.3

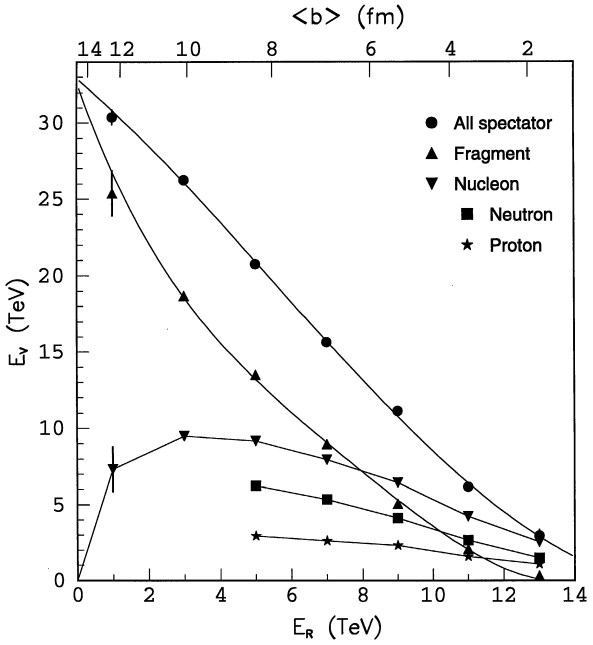

Fig. 6. Corrected forward-going energy of various species as a function of E_R. The average impact parameter scale is shown at the top. The symbols are the data points. The statistical error bars are smaller than the symbols themselves. There is an estimated systematic uncertainty of 20%. The curves through "All spectator" and "Fragment" data points are the results of polynomial fits. The polygons joining the nucleon data points are straight lines to guide the eye

The spectator composition in terms of forward-going energy is plotted as a function of E_R and of the impact parameter (as derived from Fig. 4 or Table 1) in Fig. 6. The statistical error bars are smaller than the symbols. The curves through the 'all spectator' and 'fragment' data points are the results of fourth order polynomial fits with the requirements that the total and fragment energies converge to the beam energy of 32.9 TeV at zero E_R. In central collisions ($b \approx 2$ fm), the forward-going spectator energy (2.7 TeV) is carried by about 9 neutrons, 7 protons, and, on average, 0.5 deuterons. Our result is in good agreement with a measurement in Au+Au collisions at the AGS [17], which yielded in a similar impact parameter range a forward going energy of the order of 200 GeV which translates into 182 projectile participants or, equivalently, 15 projectile spectators. At even lower (SIS) energies the ALADIN experiment reported a similar number of free spectator nucleons in central Au+Au collisions [18]. As expected the number of spectator nucleons in central nuclear collisions does not depend on the energy, it is rather determined entirely by geometry. Some aspects of the hypothesis of limiting fragmentation might be tested, if our data on the ratio of free to bound nucleons (see

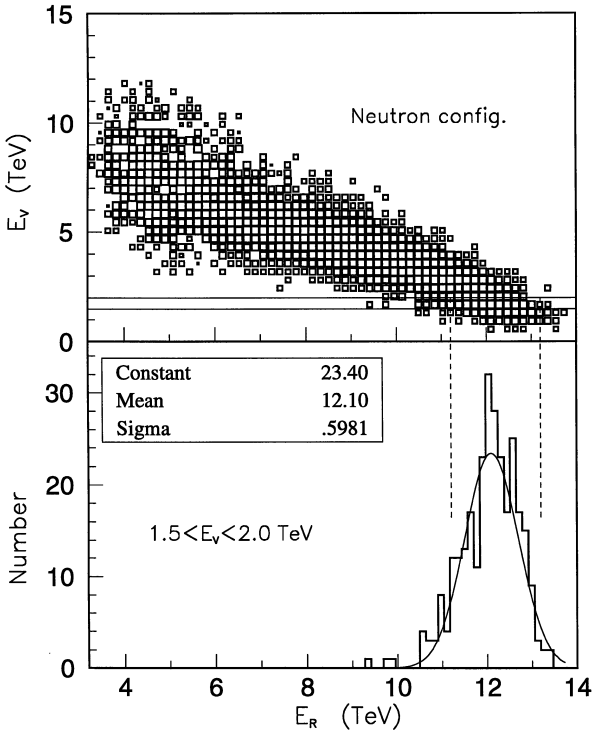

Fig. 7. An illustration of the analysis of centrality resolution, which can be deduced from the width of the Gaussian fit to the E_R distribution (lower panel) for a 0.5-TeV slice in forward-going energy (upper panel), which is fully corrected

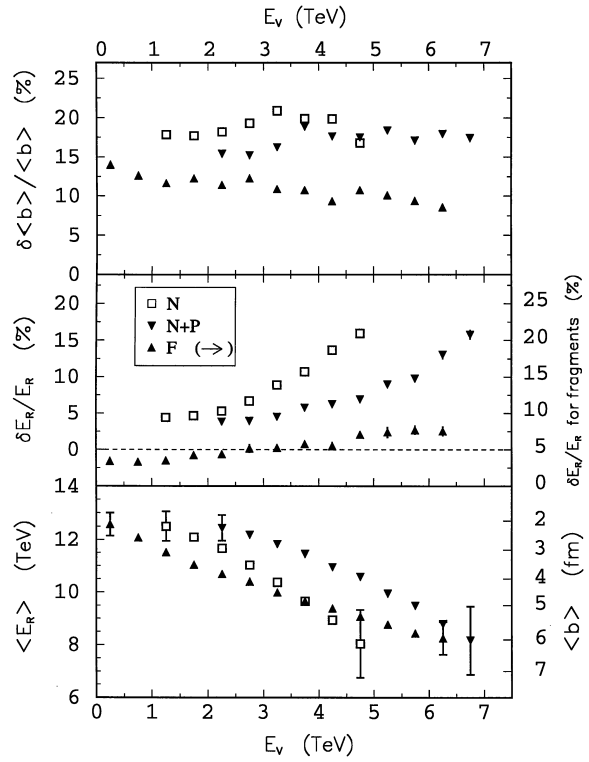

Fig. 8. Bottom: The mean $\langle E_R \rangle$ as a function of E_V for three different cases: neutrons only, nucleons, and fragments only. The average impact parameter scale is given on the right. Middle: The relative resolution of E_R as a function of E_V. The fragment points are shifted down by 5% with the scale given on the right (see arrow) in order to avoid overcrowding of data points. Top: The relative resolution of $\langle b \rangle$, which is a function of E_R estimated from Fig. 4, plotted against E_V

Fig. 6) at various impact parameters were compared to the corresponding ratios from the ALADIN experiment which are not available in this form yet. The experimental result from the light system Si+Al at AGS energy [11] falls out of the systematics oulined above: a spectator proton multiplicity of roughly one is incompatible with all other findings especially the forward energy measurement in central Au+Au collisions at similar energies [17].

The spectator fragment energy is larger than the spectator nucleon energy for $b \gtrsim 6$ fm. Large fragment energy in peripheral Pb+Pb collisions may represent survival of heavy fragments or breakup of heavy fragments into a large number of lighter fragments. The spectator energy in free nucleons first increases with impact parameter. It then decreases sharply in peripheral Pb+Pb collisions, complementing the large fragment energy.

One goal of the present fragmentation study is the determination of centrality by the use of various species of spectator matter. An important question is: Given a value of the forward-going energy of a particular species, what is the resolution of the centrality measurement? Since E_R is strongly correlated with the total energy carried by the projectile spectators (cf. Fig. 3) it is a good measure of centrality. The impact parameter resolution at a measured value of E_R can be determined using the VENUS model and comes out to be constant (0.8fm) in the range 2fm<b<12fm (cf. Fig.4). The additional loss of resolution, if only part of the forward going energy is measured (e.g. neutrons or neutrons+protons), can be deduced from the spread of the $E_R$distribution at a given value of E_V. The procedure is graphically illustrated in Fig. 7 for the spectator neutron energy. The E_R distribution for a 0.5-TeV slice of E_V is fitted by a Gaussian curve, whose mean ($\langle E_R \rangle$) and width (δE_R) allow centrality determination. The slices are made in increasing E_V until the corresponding E_R distributions are no longer Gaussian-shaped due to background contamination and/or the trigger cut. The results of this analysis for the spectator nucleon, neutron, and fragment energies are shown in Fig. 8. In the bottom panel of the figure, the mean E_R is plotted as a function of E_V with the average impact parameter scale given on the right. The middle panel of Fig. 8 shows the relative resolution of E_R, $\delta E_R/E_R$, as a function of E_V with the fragment data points being shifted down by 5% as shown by the scale on the right side in order to avoid overcrowding of data points. For central collisions, the relative resolution of E_R is about 5% with neutrons only and 4% with free nucleons. Since the average impact parameter ($\langle b \rangle$) is a function of E_R, the relative resolution of $\langle b \rangle$ is given by

$$\frac{\delta\langle b\rangle}{\langle b\rangle} = \frac{d\langle b\rangle}{dE_R}\frac{E_R}{\langle b\rangle}\frac{\delta E_R}{E_R}. \quad (3)$$

The relative resolution of $\langle b \rangle$ was calculated by fitting the average impact parameter as a function of E_R in Fig. 4. This resolution is displayed in the top panel of Fig. 8. In central collisions, the relative resolution of $\langle b \rangle$ is about 19% for the spectator neutron energy, 15% for the nucleon energy, and 12% for the fragment energy. The variation in $\delta\langle b \rangle / \langle b \rangle$ as a function of E_V is small for all three cases. The intrinsic spread of the impact parameter of about 0.8 fm which was mentioned earlier is not included in the values shown in the top panel of Fig. 8.

5 Conclusion

The composition of projectile spectator matter in Pb+Pb collisions at SPS energy was measured for various impact parameters. The different measurements of forward-going energy are internally consistent within the systematic uncertainty of 20%. In central collisions, there are approximately 9 spectator neutrons, 7 protons, and half a deuteron. On the other hand, fragments dominate the spectator matter in peripheral collisions. The relative resolution of the average impact parameter obtained using only the spectator neutrons and neutrons+protons in central collisions is 19% and 15%, respectively.

References

1. T. Alber, *et al.*, Phys. Rev. Lett. **75**, 3814 (1995)
2. H.H. Heckman, *et al.*, Phys. Rev. Lett. **28**, 926 (1972)
3. D.E. Greiner, *et al.*, Phys. Rev. Lett. **35**, 152 (1975)
4. J. Benecke, *et al.*, Phys. Rev. **188**, 2159 (1969)
5. J.V. Geaga, *et al.*, Phys. Rev. Lett. **45**, 1993 (1980)
6. S.B. Kaufman, *et al.*, Phys. Rev. C **22**, 1897 (1980)
7. D.L. Olson, *et al.*, Phys. Rev. C **28**, 1602 (1983)
8. W.B. Christie, *et al.*, Phys. Rev. C **48**, 2973 (1993)
9. G.J. Kunde, *et al.*, Phys. Rev. Lett. **74**, 38 (1995)
10. A. Schüttauf, *et al.*, Nucl. Phys. A **607**, 457 (1996)
11. J. Barrette *et al.*,Phys. Rev. C45, 819 (1992)
12. M.L. Cherry, *et al.*, Phys. Rev. C **52**, 2652 (1995)
13. B. Berthier, *et al.*, Phys. Lett. B **193**, 417 (1987)
14. P.Alvarez de Lara, *et al.*, Phys. Lett. B **351**, 418 (1995)
15. R. Brun, *et al.*, GEANT Detector Description and Simulation Tool, CERN, Genva 1993 (unpublished)
16. K. Werner, Phys. Rept. **232**, 87 (1993)
17. F. Wang for the E802 collaboration, Proceedings of HIPAGS '96, WSU-NP-96-16
18. C. Gross, PhD thesis, University Frankfurt, 1998